2007-05-02

Use of the Clegg Impact Soil Tester to Access Rutting Susceptiblity of Cement-Treated Base Material Under Early Trafficking

Garth B. Reese
Brigham Young University - Provo

USE OF THE HEAVY CLEGG IMPACT SOIL TESTER TO ASSESS RUTTING SUSCEPTIBILITY OF CEMENT-TREATED BASE MATERIAL UNDER EARLY TRAFFICKING

by

G. Benjamin Reese

A thesis submitted to the faculty of

Brigham Young University

in partial fulfillment of the requirements for the degree of

Master of Science

Department of Civil and Environmental Engineering

Brigham Young University

December 2007

BRIGHAM YOUNG UNIVERSITY

GRADUATE COMMITTEE APPROVAL

of a thesis submitted by

G. Benjamin Reese

This thesis has been read by each member of the following graduate committee and by majority vote has been found to be satisfactory.

Date	W. Spencer Guthrie, Chair
Date	Grant G. Schultz
Date	Kyle M. Rollins

BRIGHAM YOUNG UNIVERSITY

As chair of the candidate's graduate committee, I have read the thesis of G. Benjamin Reese in its final form and have found that (1) its format, citations, and bibliographical style are consistent and acceptable and fulfill university and department style requirements; (2) its illustrative materials including figures, tables, and charts are in place; and (3) the final manuscript is satisfactory to the graduate committee and is ready for submission to the university library.

Date	W. Spencer Guthrie Chair, Graduate Committee

Accepted for the Department

E. James Nelson
Graduate Coordinator

Accepted for the College

Alan R. Parkinson
Dean, Ira A. Fulton College of Engineering and Technology

ABSTRACT

USE OF THE HEAVY CLEGG IMPACT SOIL TESTER

TO ASSESS RUTTING SUSCEPTIBILITY OF

CEMENT-TREATED BASE MATERIAL

UNDER EARLY TRAFFICKING

G. Benjamin Reese

Department of Civil and Environmental Engineering

Master of Science

In order to avoid the occurrence of early-age damage, cement-treated base (CTB) materials must be allowed to cure for a period of time before the pavement can be opened to traffic. Trafficking of a CTB before sufficient strength gain has occurred can lead to marring or rutting of the treated layer. The specific objectives of this research were to examine the correlation between Clegg impact values (CIVs) determined using a heavy Clegg impact soil tester and rut depths measured in newly constructed CTB and subsequently establish a threshold CIV at which rutting should not occur.

The experimental work included field testing at several locations along United States Highway 91 near Smithfield, Utah, and laboratory testing at the Brigham Young University (BYU) Highway Materials Laboratory. In both the field and laboratory test programs, ruts were created in CTB layers using a specially manufactured heavy wheeled rutting device (HWRD). In the field, ruts caused by repeated passes of a

standard pickup and a water truck were also evaluated. The collected data were analyzed using regression to identify a threshold CIV above which the CTB should not be susceptible to unacceptable rutting.

From the collected data, one may conclude that successive wheel passes each cause less incremental rutting than previous passes and that CTB similar to the material tested in this research should experience only negligible rutting at CIVs greater than about 35. The maximum rut depth measured in either field or laboratory rutting tests was less than 0.35 in. in this research, probably due to the high quality limestone base material utilized to construct the CTB.

In identifying a recommended threshold CIV at which CTB layers may be opened to early trafficking, researchers proposed a maximum tolerable rut depth of 0.10 in. for this project, which corresponds to a CIV of approximately 25. Because a CIV of 25 is associated with an acceptably minimal rut depth even after 100 passes of the HWRD, is achievable within a reasonable amount of time under normal curing conditions, and is consistent with earlier research, this threshold is recommended as the minimum average value that must be attained by a given CTB construction section before it can be opened to early trafficking. Use of the proposed threshold CIV should then ensure satisfactory performance of the CTB under even heavy construction traffic to the extent that the material properties do not differ greatly from those of the CTB evaluated in this research.

ACKNOWLEDGEMENTS

The author acknowledges the help of Dr. Spencer Guthrie in planning and carrying out this project. Support for this project was provided by the Utah Department of Transportation and the Portland Cement Association. The BYU Precision Machining Laboratory constructed the heavy wheeled rutting device used in this research. Dr. Grant Schultz and Dr. Kyle Rollins are recognized for their participation on the graduate committee. BYU students Adam Birdsall, Aimee Birdsall, Ash Brown, Rebecca Crane, Benjamin Griggs, Maile Rogers, and Matt Roper assisted with this testing. Lastly, the author wishes to thank his wife and son, who have been extremely supportive in helping him accomplish this stage of his education.

TABLE OF CONTENTS

LIST OF TABLES

LIST OF FIGURES

CHAPTER 1
INTRODUCTION

1.1 PROBLEM STATEMENT

Many agencies routinely specify the use of cement-treated base (CTB) for both asphalt and concrete pavements. As Portland cement cures over time, it forms chemical compounds that bind the aggregate particles together. However, because cement cures at different rates depending on the ambient air temperature and humidity, wind speed, type of cement used, and concentration of cement used, exactly predicting the length of curing time required before CTB may be trafficked is difficult (*1*). If the CTB has cured sufficiently, then heavy construction vehicles, such as water and distributor trucks that can weigh up to 60,000 lbs, can safely travel over the CTB with no risk of permanently damaging it. However, in the event that the CTB has not cured sufficiently, such heavy construction traffic can create ruts in the CTB.

To protect their investments, many agencies select curing times up to 7 days, for example, that overestimate the actual time needed for the CTB to gain sufficient strength that it can be opened to trafficking (*2, 3*). This conservative approach does protect the public investment, but it also, at times, unnecessarily wastes valuable time and money on the part of the construction contractors who must wait for the specified time to expire before continuing work on the project.

As an alternative to specifying a curing time, engineers may specify field testing of CTB. Several devices are currently available for evaluating the stiffness of CTB materials in the field, including the soil stiffness gauge (SSG), heavy Clegg impact soil tester (CIST), dynamic cone penetrometer (DCP), portable falling-weight deflectometer (PFWD), and falling-weight deflectometer (FWD), for example. Previous researchers at Brigham Young University (BYU) evaluated these instruments based on their sensitivity to curing time, repeatability, efficiency, ruggedness, ease of use, and cost and recommended use of the CIST for assessing early-age strength gain of CTB layers (*2*).

A CIST, commonly called a Clegg hammer, outputs a Clegg impact value (CIV) that ranges between 1 for low stiffness and 200 for higher stiffness(*4*). However, while CIVs typical of various types of aggregate base materials have been measured, no threshold CIV has yet been established for opening CTB layers to early trafficking (*2, 5*). Furthermore, the relationship between CIVs and CTB rutting susceptibility has not been previously investigated. Therefore, the specific objectives of this research were to examine the correlation between CIVs and rut depths in newly constructed CTB and subsequently establish a threshold CIV at which unacceptable rutting should not occur.

1.2 SCOPE

In cooperation with the Utah Department of Transportation (UDOT), research personnel at BYU performed field testing at several locations along United States Highway 91 (US-91) near Smithfield, Utah. This testing was completed during the summer months of 2005 when the ambient air temperature was relatively high and the ambient relative humidity was relatively low. Additional testing was conducted at the BYU Highway Materials Laboratory. In both the field and laboratory test programs, ruts were created in CTB layers using a specially manufactured heavy wheeled rutting device (HWRD) that imparted a contact pressure equal to that caused by an equivalent single axle load (ESAL). In the field, ruts caused by repeated passes of a water truck and a standard pickup truck were also evaluated. For consistency, a limestone aggregate treated with 2.0 percent Portland cement by weight of dry aggregate was utilized for both the field and laboratory test programs.

1.3 OUTLINE OF REPORT

This report contains five chapters. Chapter 1 presents the objectives and scope of the research. Chapter 2 provides information concerning CTB construction, testing, and rutting. Descriptions of the experimental plan, field and laboratory testing procedures, and data analysis methods are given in Chapter 3. Test results are explained in Chapter

4 together with a discussion of the research findings. In Chapter 5, summaries of the procedures, research findings, and recommendations are presented.

CHAPTER 2
BACKGROUND

2.1 OVERVIEW

The following sections discuss current CTB construction methods, use of the CIST for CTB testing, and CTB rutting.

2.2 CTB CONSTRUCTION

Base courses are typically imported aggregates that are placed by dump truck on a prepared subgrade and then graded and compacted following project specifications (*6*, *7*). When the available aggregates exhibit inadequate strength or durability, design engineers may specify the use of cement stabilization. Cement has been used as a soil and aggregate stabilizer since 1935 (*8*). The cement powder is trucked to either the road construction site or a batch plant for blending with the aggregate in quantities typically ranging between 1 and 6 percent by dry weight of aggregate (*9*, *10*). The CTB material should be prepared at its optimum moisture content (OMC), which should be predetermined in a geotechnical testing laboratory; OMCs generally vary between 5 and 15 percent water, measured by dry weight of aggregate and cement (*8*).

In the field, cement in powder or slurry form is spread directly onto the aggregate base layer. A single traverse-shaft rotary mixer, or reclaimer, is often used to mix the cement into the base material (*7, 8*). Water from a water truck working in tandem with the reclaimer can be added directly into the mixing chamber of the reclaimer when the in situ water content is lower than the OMC. Figure 2.1 shows a reclaimer and water truck in operation at one of the US-91 reconstruction sites included in this research.

After the CTB has been placed on the roadway, it should be compacted, graded, and cured. To ensure that the CTB retains sufficient moisture for continued cement hydration, the base should be watered periodically. Watering should continue until a

FIGURE 2.1 Reclaimer and water truck.

prime coat, typically a bituminous cutback or emulsion, is placed on the CTB in preparation for an asphalt or concrete wearing course (*7*, *8*).

Because water and distributor trucks can weigh up to 60,000 lbs, the CTB may experience marring or rutting under repeated passes of such construction traffic if it is not allowed to cure sufficiently beforehand. Rutting occurs as the void space between aggregate particles is reduced under heavy loading. Densification in the wheel paths is often accompanied by the occurrence of upward shoving of aggregate particles on both sides of the passing wheel. Such damage can occur with a single pass of a heavy vehicle and only becomes more severe with repeated passes of heavy wheel loads. If excessively damaged, the CTB layer may need to be replaced before the wearing course can be constructed.

The longer a CTB material cures, the more resistant to damage it becomes. However, as stated earlier, the rate of strength development depends on the ambient air temperature and humidity, wind speed, type of cement used, and concentration of cement used, making determinations of curing time requirements difficult (*1*). Because waiting a specified period of time for the CTB to cure is not efficient, agencies need a simple test that can be used to determine whether or not a particular CTB section can be opened to early trafficking at a particular time.

2.3 CTB TESTING

With the support of the UDOT and the Portland Cement Association (PCA), previous BYU researchers assessed the utility of five different instruments available for measuring CTB stiffness in the field. The research included the SSG, heavy CIST, DCP, PFWD, and FWD, which were evaluated at four sites along Interstate 84 near Morgan, Utah, and at three sites along US-91 near Richmond, Utah. These instruments were evaluated in terms of their sensitivity, repeatability, efficiency, ruggedness, ease of use, and cost. Sensitivity was defined in the research as the degree to which instrument readings were correlated to CTB curing time. Repeatability was the relative proximity of repeated measurements to each other. Efficiency reflected the number of readings required to estimate the true value, or population mean, from the sample mean at specified tolerance and reliability levels. Ruggedness described the degree to which instrument readings were influenced by small variations in procedures or other testing conditions. Ease of use reflected the simplicity, speed, and operator comfort associated with instrument use (*2*).

Overall, the CIST was determined to be the most sensitive to curing time and the most repeatable, and it required the fewest readings to acquire reliable results. In addition, the CIST was shown to exhibit the least sensitivity to small variations in testing conditions and was the simplest and quickest to use. Finally, the CIST was also reported as being less expensive than the SSG, PFWD, and FWD, which adds an economic incentive as another basis for recommending its use. For these reasons, the CIST was recommended as the best tool for monitoring early-age strength gain of CTB layers (*2*).

The CIST was originally invented by an engineer named Baden Clegg for the purpose of evaluating low-traffic roads in Western Australia (*5*). These roads consisted of an aggregate base layer surfaced with only a prime coat. A method was needed for testing base materials in the field that could be correlated with common strength tests such as the California bearing ratio test, Texas triaxial test, and Benkelman beam test. In particular, the field CBR test had become very popular immediately following World

War II, but it was cumbersome and time-consuming to perform. Clegg invented the CIST for the purpose of replacing the field CBR test (*5, 11, 12*).

The CIST consists of a drop weight instrumented with an accelerometer and confined within a thin-walled cylindrical metal guide tube. The basic principal that governs the functionality of the CIST is that the deceleration of a dropped body is directly related to the stiffness and shear resistance offered by the material that the body strikes (*12*). When the weight is dropped on a base layer, the aggregate matrix decelerates the weight through the occurrence of shear deformation and/or densification, which are, conveniently, the same factors that influence the rutting behavior of CTB. The accelerometer mounted on the CIST weight measures the peak deceleration of the weight as it strikes the aggregate surface. A digital display unit reports this measurement in terms of a CIV, where 1 CIV is equivalent to 10 times the acceleration rate of gravity. That is, if a CIV of 25 was obtained on a particular aggregate layer, the drop weight of the CIST would have decelerated at 250 times the acceleration rate of gravity. Four successive blows of the hammer at the same location constitute one test, which can be completed in less than 30 seconds by a single operator (*13, 14, 15*).

CISTs are available in three primary configurations: the standard CIST, the light CIST, and the heavy CIST. The standard CIST was developed first and consists of a 10-lb weight that falls a distance of 18 in (*13, 14*). The light CIST is available in two versions consisting of either a 2.5-lb or a 5.0-lb weight that falls a distance of 12 in. The heavy CIST, which is the focus of this research, is comprised of a 44-lb drop weight that falls a distance of 12 in. Due to its higher weight, the heavy CIST is recommended for evaluating compacted aggregate base and subgrade materials (*13, 14*). The depth of interrogation may be estimated to be about two times the diameter of the drop weight, or about 12 in. for this hammer (*2, 11*). The heavy CIST is shown in Figure 2.2.

Following his development of the standard CIST, Clegg performed extensive research investigating variability in CIV within a construction section, correlations between CIV and CBR, and relationships between CIV and long-term pavement performance. He found that within the width of a roadway the CIVs could range between less than 30 and more than 60, depending on the quality of compaction, and that a CIV of 30 was approximately equal to a CBR of 50 (*5*). Base materials with CIVs

FIGURE 2.2 CIST on CTB.

between about 10 and 45 exhibited poor long-term performance, while those with higher CIVs provided satisfactory performance under the traffic loads and environmental conditions typical of the sites he tested (*5, 11*). In subsequent years, a protocol for the use of the standard CIST has been developed and is detailed in American Society for Testing and Materials (ASTM) D 5874 (Standard Test Method for Determination of the Impact Value (IV) of a Soil).

To facilitate application of these values measured using the standard CIST to sites tested using the heavy CIST, Clegg later reported that 1 CIV obtained using the heavy CIST is equal to a CIV of between 0.50 and 0.62 using the standard CIST (*15*). Therefore, the threshold CIV of 45 mentioned previously, which is associated with the standard CIST, is equal to a CIV of between 23 and 28 measured using the heavy CIST. Because the heavy CIST was utilized in this research, these data, although purely empirical and site-specific, were compared against the test results reported in Chapter 4 of this report in the process of developing a threshold value at which CTB layers may be opened to early trafficking.

2.4 CTB RUTTING

An exhaustive literature review was performed on the subject of CTB and rutting. Published research addresses such topics as long-term CTB performance, efficacy of cement stabilization for improving different soil types, effects of reclaimed asphalt pavement in CTB, optimal CTB mixing and curing conditions, and various other characteristics of CTB (*10*, *16*, *17*, *18*, *19*, *20*, *21*, *22*, *23*, *24*, *25*, *26*, *27*). However, beyond the research performed at BYU, which is detailed in the previous section, the literature lacks information concerning early-age CTB properties, including rutting characteristics of CTB under early trafficking. That is, excluding the systems developed in the current project, no methods or thresholds have been developed for assessing the susceptibility of CTB to rutting under early trafficking.

Nonetheless, an erosion threshold for CTB and several rut depth thresholds associated primarily with asphalt are given in Table 2.1, which also shows the agencies that developed the specifications. The South African wheel tracker erosion test simulates the occurrence of abrasion on CTB surfaces (*24*), while the Hamburg wheel tracking device measures the rutting susceptibility of asphalt beam specimens (*28*). The Asphalt Institute rut depth threshold was used by that organization in developing transfer functions relating vertical compressive strains in pavements to service life, where rut depths equal to or exceeding 0.5 in. denote pavement failure. Although most of the test procedures listed in Table 2.1 require many more wheel passes than would be expected on an unsurfaced CTB during the first few days of curing, these data were consulted in development of a threshold CTB rut depth specific to this research.

TABLE 2.1 Rut Depth Thresholds (*24, 28, 29*)

Test Type	Agency	Wheel Passes	Rut Depth Threshold (in.)
South African Wheel Tracker Erosion Test for CTB	South Africa	5,000	0.04
Hamburg Wheel Tracking Test for Asphalt Concrete	Federal Highway Administration	10,000	0.16
	Federal Highway Administration	20,000	0.39
	City of Hamburg, Germany	19,200	0.04
	Utah Department of Transportation	20,000	0.59
Performance Specification for Asphalt Concrete	Asphalt Institute	Life	0.50

2.5 SUMMARY

When available aggregate base materials exhibit inadequate strength or durability, design engineers may specify the use of cement stabilization. In order to avoid the occurrence of early-age damage, CTB materials must be allowed to cure for a period of time before the layer can be opened to early trafficking. Trafficking of a cement-treated material before sufficient strength gain has occurred can lead to marring or rutting of the layer. Such damage can occur with a single pass of a heavy vehicle and only becomes more severe with repeated passes of heavy wheel loads.

Previous research recommended use of the heavy CIST for assessing early-age strength gain of CTB, although no threshold CIV was developed. CIV has been correlated to both CBR and long-term pavement performance by other researchers, but the relationship between CIV and rutting of CTB layers under early trafficking has not been previously investigated. The exhaustive literature review conducted in this research yielded very limited information on this topic, justifying the need for additional work as described in Chapter 3.

CHAPTER 3

EXPERIMENTAL METHODOLOGY

3.1 OVERVIEW

This research included both field and laboratory testing. In both cases, the testing involved forming ruts in newly constructed CTB and then measuring CIVs in the immediate vicinity of the rut locations. Laboratory testing also included unconfined compressive strength (UCS) testing of CTB specimens. This chapter contains a description of the HWRD that was specially manufactured for creating ruts in CTB, as well as explanations of both the field and laboratory testing procedures and data analyses utilized in the research.

3.2 HWRD CONSTRUCTION AND USE

As stated in Chapter 2, while test protocols are available for evaluating the susceptibility of asphalt mixtures to rutting (*24*, *28*, *30*), no standard methods have been developed for assessing the rutting characteristics of CTB materials. Therefore, the HWRD was designed by BYU researchers specifically for this research, and measurement protocols were prepared to facilitate consistent measurements of rut depths both in the field and in the laboratory using the device.

In designing the HWRD, the researchers desired to simulate the contact pressure typical of an ESAL while minimizing the total weight of the device to ensure adequate ease of use. The resulting product consists of two 1-in.-thick plate-metal wheels, each having a diameter of 12 in. The wheels are joined by an axle comprised of a 1-in.-diameter steel rod 18 in. in length. A small lip on each end of the axle prevents the wheels from traveling inward during use. Outward movement of the wheels is arrested by a small clip that slides over the end of the rod once the wheel is in place. Between the wheels, the axle has two flattened sides along its length, which are parallel to each other and allow weights to be hung on the axle in such a manner that the weights cannot rotate relative to each other as the HWRD is rolled. The ends of the axle are lubricated to facilitate free rolling action of the wheels. Two HWRDs were constructed by personnel at the BYU Precision Machining Laboratory and are shown in Figure 3.1.

The HWRD weighs approximately 60 lbs without any weights placed on the axle. However, during use, a set of four 35-lb soil consolidometer weights are hung from the axle to produce a total load of 200 pounds; this configuration is depicted in Figure 3.2. Assuming the footprint of each of the HWRD wheels is approximately 1 in.^{2} when placed on a CTB surface, the pressure imparted to the CTB is approximately 100 psi, equal to the contact pressure associated with an ESAL. The HWRD creates depressions in the CTB as it is manually rolled over the CTB surface in a series of successive passes. For example, the lower portion of Figure 3.2 shows the shallow ruts created by the HWRD at that test location.

Because a single wheel of an ESAL carries a load of 4500 lbs compared to a load of 100 lbs carried by a single wheel of an HWRD, the distributions of vertical stress become increasingly different with increasing depth below the CTB surface. Figure 3.3

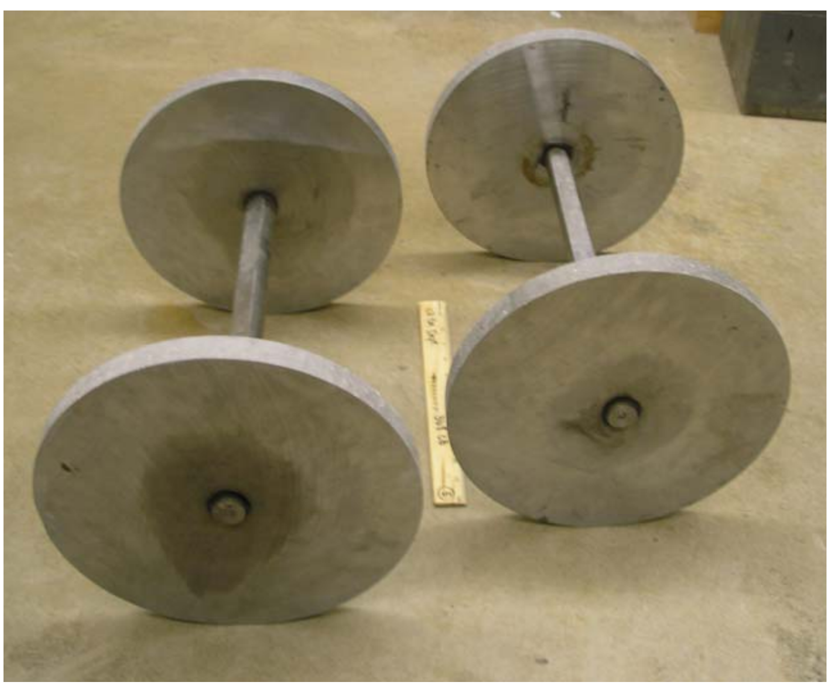

FIGURE 3.1 HWRDs.

FIGURE 3.2 HWRD with four 35-lb weights.

displays the vertical stress profiles associated with the HWRD and an ESAL. The stress profiles were computed using KENLAYER software and assuming a modulus and Poisson's ratio of 200 ksi and 0.15, respectively, for the CTB (*29*). In previous research conducted on US-91, this level of stiffness was achieved by the CTB after 2 or 3 days of curing and is equivalent to a CIV of approximately 25 (*2*). Because of their relevance to this research, the vertical stress profiles for a water truck and a standard pickup truck are also shown in the figure. In this case, the wheel load and contact pressure were assumed to be 6,000 lbs and 100 psi, respectively, for the water truck and 2,000 lbs and 80 psi, respectively, for the pickup.

Although the vertical stress profiles displayed in Figure 3.3 show that the HWRD does not produce the same level of stress as typical heavy traffic loads, they do show that the vertical stresses induced by the HWRD are between those induced by an ESAL and a pickup truck within the upper 0.5 in. of CTB, where rutting is most likely to occur.

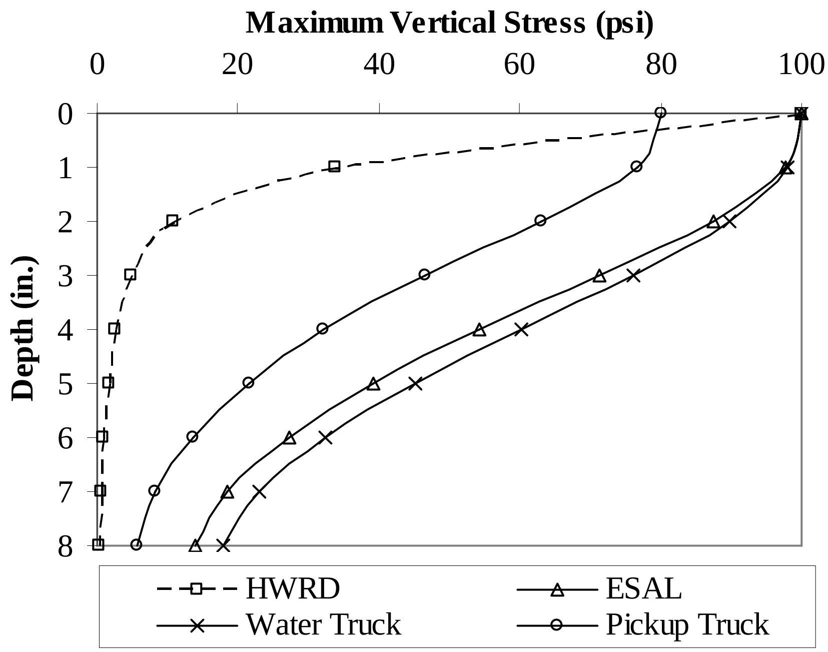

FIGURE 3.3 Vertical stress profiles in CTB.

To facilitate consistent and precise measurements of rut depth, a special measuring board system (MBS) was constructed for this research. The MBS consists of a wooden beam about 4 ft in length with a cross-section having dimensions of approximately 4 in. by 4 in., metal support blocks for the ends of the beam, a micrometer having a resolution of 0.001 in., and approximately 0.5-in.-diameter metal disks for placement in the bottom of the rut to prevent penetration of the tip of the micrometer into the CTB during testing. The beam rests horizontally on the support blocks as shown in Figure 3.4, and the micrometer is mounted in the beam, in turn, at two locations corresponding to the locations of the ruts made by the HWRD wheels. The support blocks remain in their original positions during each test setup to ensure a constant datum, but the beam is removed to facilitate successive passes of the HWRD over the test site immediately between the blocks. When a measurement of rut depth is desired, the beam is returned to its place on the blocks, and the micrometer is used to measure the distance from its place in the beam to the top surface of each circular disk, as demonstrated in Figure 3.5. The disks are removed and replaced between sets of passes,

FIGURE 3.4 MBS components.

FIGURE 3.5 Micrometer with metal disk.

and actual rut depths are computed for each wheel path by subtracting the original micrometer reading from each successive micrometer reading.

3.3 FIELD TESTING

Field testing was conducted at several sites along US-91 between the cities of Smithfield and Richmond in northern Utah during the summer of 2005. A photograph of a typical site is shown in Figure 3.6, and a map of the facility in this region is given in Figure 3.7. The weather at the test sites was mostly sunny during testing, with average daytime temperatures between 81°F and 89°F and relative humidity between 33 and 40 percent.

The highway in this region was completely reconstructed as part of a widening project. At this location, US-91 was originally a composite pavement comprised of a concrete layer overlain by asphalt. The reconstruction plan required milling and removal of the original asphalt layer and rubblization of the underlying concrete, which was then bladed to the side of the road. The original base layer and subgrade were then excavated

FIGURE 3.6 US-91 site picture.

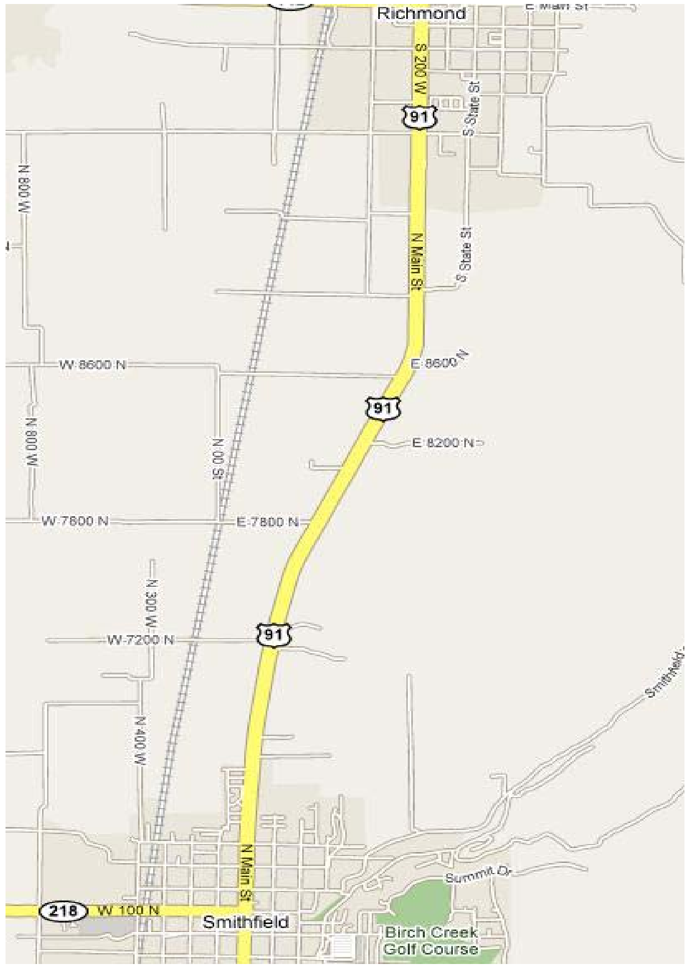

FIGURE 3.7 Map of US-91 (*31*).

an additional 2 ft below the bottom of the original concrete layer in order to facilitate a thicker pavement structure upon reconstruction.

Once the excavation was completed, the rubblized concrete was bladed back onto the roadway, compacted on top of the newly exposed subgrade, and overlain with an 8-in. layer of comparatively high quality limestone base material. This material is classified as A-1-a according to American Association of State Highway and Transportation Officials M-145 (Standard Specification for Classification of Soils and Soil-Aggregate Mixtures for Highway Construction Purposes) and as SW-SM (well-graded sand with silt and gravel) according to ASTM D 2487 (Standard Classification of Soils for Engineering Purposes (Unified Soil Classification System)). The washed particle-size distribution for the limestone is given in Figure 3.8. Following initial

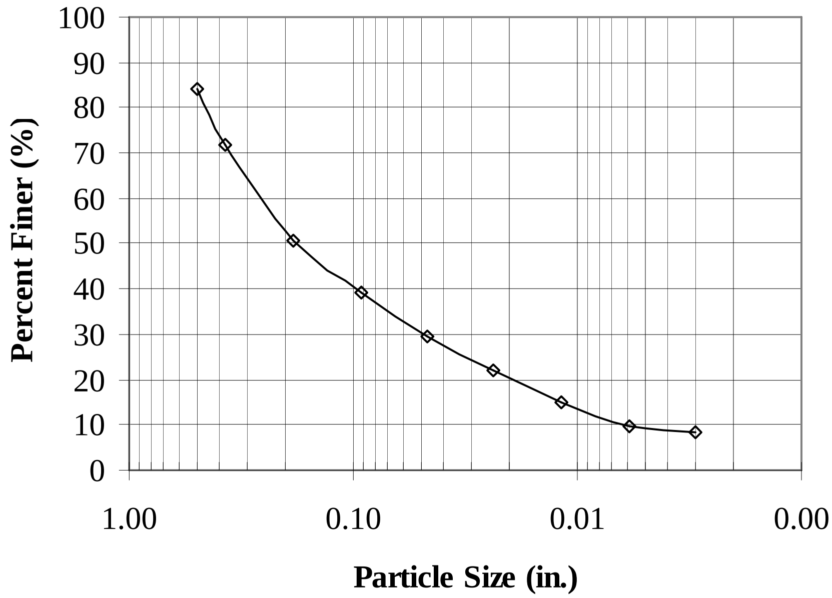

FIGURE 3.8 Particle-size distribution for limestone base material.

compaction, 2.0 percent Portland cement by weight of dry aggregate was placed with a spreader and then mixed with the base material using a reclaimer to form the CTB. The full depth of the granular base layer was treated to achieve an 8-in-thick CTB. Water was introduced during CTB mixing, and compaction followed immediately afterwards. The CTB was compacted to between 85 and 88 percent of its maximum dry density (MDD), which was determined in the laboratory to be 137.8 pcf at an OMC of 7.0 percent using modified Proctor effort (*16, 17*). The material was then graded to project specifications.

In cooperation with the construction contractor, the researchers selected several CTB test sites, some freshly compacted and others having cured for a few days, to ensure that the testing would yield a full range of results. Sample CIVs were measured at potential sites to evaluate the suitability of each location prior to conducting rut testing. When a suitable location was identified, two teams of two persons each set up the testing equipment, including a HWRD with weights and an MBS, at each of two testing sites as depicted in Figure 3.9. The researchers were careful not to disturb intended test sites by avoiding walking on or rolling the HWRD or CIST over them during the process of unloading equipment.

FIGURE 3.9 Layout of field test site.

To perform the testing, researchers situated the support blocks on either side of the intended test site and aligned the wooden beam along marks on the top surfaces of the blocks. The metal disks were placed directly beneath the micrometer mounting locations in the beam, and initial micrometer readings were recorded, with two replicate measurements taken in each wheel path. The loaded HWRD was then rolled up to the MBS so that the wheels were aligned with the micrometer mounting locations in the beam. With the HWRD properly situated, the beam was removed, and the HWRD was manually rolled over the surface in sets of 10 passes each. A pass consisted of one traverse of the wheels. One operator propelled the HWRD, while the other steadied the weights so that they did not drag on the ground. Both operators were careful to ensure that the wheels stayed in their designated paths throughout the rutting process.

Following completion of the first set of 10 wheel passes, the MBS was again placed on the support blocks, the metal disks were placed in the ruts, and two micrometer readings were taken in each wheel path. Five sets of 10 passes were followed by one set of 50 passes for a total of 100 passes per test site. At the conclusion of this rutting procedure, CIVs were measured following the guidelines set forth in ASTM D 5874 at three locations immediately adjacent to each wheel path.

To minimize variability in the testing, the same person on each team always operated the micrometer and the CIST, while the other person recorded the data. If a support block was disturbed during the rutting process due to operator error or any other reason, the test was considered void and discarded. A total of 43 individual field sites were tested in this research.

In addition to testing using the HWRD, rut testing was also performed using both a water truck and a standard pickup truck. The water truck weighed approximately 60,000 lbs. The front axle of the truck was assumed to carry 12,000 lbs, while the remaining 48,000 lbs was assumed to be distributed over the tandem rear axles consisting of a total of eight wheels. The pickup truck had four wheels and weighed approximately 7,000 lbs, with the front axle carrying nearly 4,000 lbs. The testing procedure for these vehicles was similar to that developed for the HWRD. Because both vehicles were wider than the length of the MBS, however, a longer wooden beam was utilized instead. After the initial micrometer readings were recorded at each site, the operators drove the trucks back and forth until 10 passes were completed. Due to limited availability of contractor assistance for this task, rut depths resulting from more than 10 passes of the trucks were not evaluated. Figures 3.10 and 3.11 depict the water truck and pickup truck setups, respectively. The longer MBS utilized in each case is displayed in the figures.

FIGURE 3.10 Water truck test setup.

FIGURE 3.11 Pickup truck test setup.

3.4 LABORATORY TESTING

To facilitate evaluation of the relationship between CIV and CTB rutting in a more controlled environment, a wooden box made of plywood and structural lumber with nominal cross-section dimensions of 2 in. by 12 in. was constructed in the BYU Highway Materials Laboratory. The inside of the box was 27 in. wide by 55 in. long by 11 in. deep, large enough to allow three separate rutting tests to be performed. After being constructed, the box was lightly wetted and filled with a cement-treated granular base material similar to that utilized in the reconstruction of US-91. Before being placed in the box, the material was mixed at OMC in a portable concrete mixer with 2.0 percent cement by weight of dry aggregate. After being thoroughly mixed, the material was deposited into a wheelbarrow and transferred in approximately 3-in. lifts into the box as shown in Figure 3.12. The material was then spread to the corners of the box with a rake.

Once the material was uniformly distributed in the box, the CTB was densified using a jumping-jack compactor, and manually operated modified Proctor hammers were utilized to compact the material along the edges of the box where the jumping-jack compactor was not as effective. To ensure a smooth surface on the final lift, small steel blocks were used to strike down any irregularities in the CTB surface. A sheet of plastic was then placed over the CTB to ensure adequate curing, which occurred at an ambient laboratory temperature of approximately 70°F.

Testing identical to that performed with the HWRD in the field was performed at time intervals of 2, 4, and 8 hours following final compaction of the CTB. To enable more direct correlations between measured rut depths and CIVs, however, rut depths were measured separately at each of the three CIST test locations. The positions of the support blocks were therefore carefully marked on the sides of the box to ensure precise placement of the MBS in each case. The approximate locations of the MBS placements, wheel paths, and CIST tests are shown in Figure 3.13. In the figure, wheel paths that were rutted at the same curing time with a single HWRD are marked with the same letter, and CIST test locations and rut measurement locations that were paired together are labeled with the same numeral. A total of 18 CIVs were measured with this layout, with rut depths measured after 10, 20, 30, 40, 50, and 100 wheel passes.

FIGURE 3.12 Preparation of laboratory box specimen.

Figure 3.14 shows the laboratory box specimen after the testing was completed. Following the rutting and CIST testing, a nuclear density gauge was used to measure the spatial variability in density within the CTB specimen. Six locations were tested and showed a satisfactory range in relative density of 96 to 98 percent of the MDD.

In addition to the rutting data, UCS data were also collected for the CTB material evaluated in this laboratory research. The purpose of the testing was to facilitate comparison of CIVs with a more commonly used measure of CTB strength. Specimen compaction was performed using the modified Proctor procedure to create 4-in.-diameter specimens with a target height of 4.6 in. Described in ASTM D 1557 (Standard Test Methods for Laboratory Compaction Characteristics of Soil Using Modified Effort (56,000ft-lbf/ft3 (2,700 kN-m/m3))) Method B, the modified Proctor procedure requires

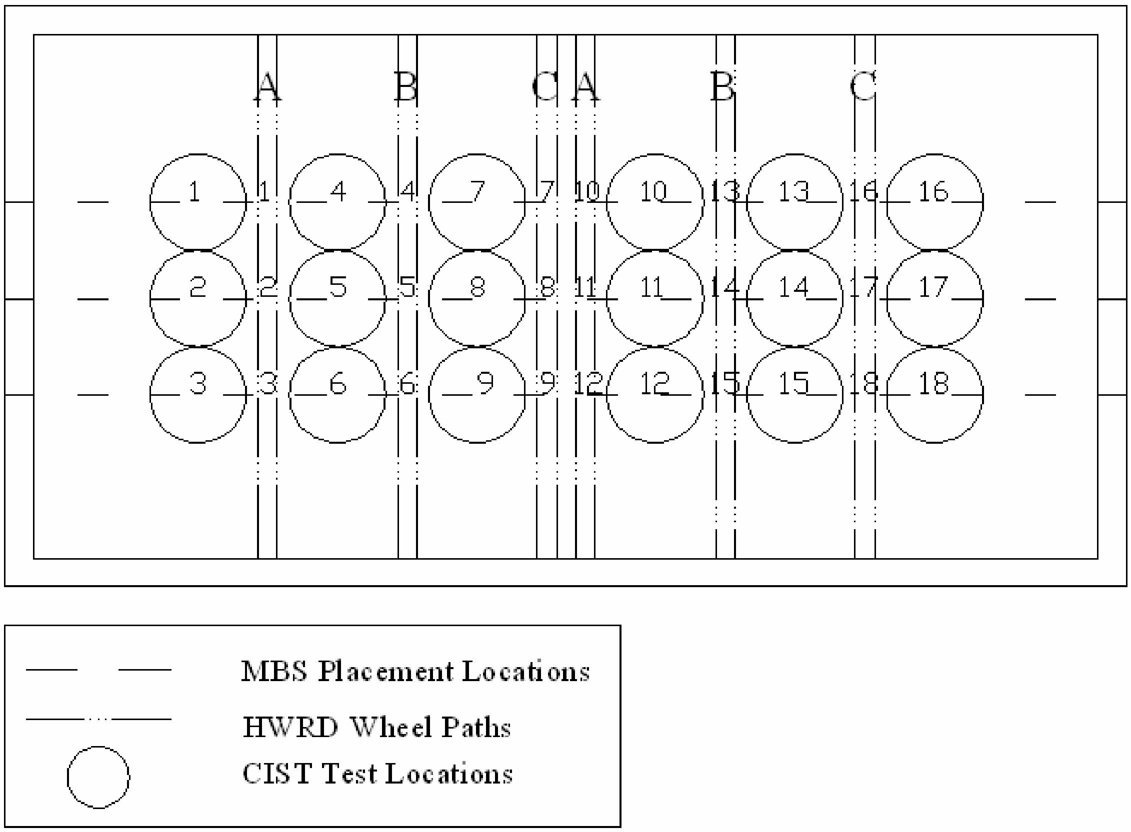

FIGURE 3.13 Layout of tests on laboratory box specimen.

compaction of specimens in five lifts of 25 blows per lift with a 10-lb hammer dropped from a height of 18 in. The specimens were compacted, on average, to 99 percent of the MDD.

Following compaction, the specimens were extruded and cured for 2, 4, or 8 hours, corresponding with the testing times utilized for the laboratory rut testing, in the same environment as the box specimen. The specimens were then capped with a high-strength gypsum compound and subjected to compression testing at a constant strain rate of 0.05 in./minute in accordance with ASTM D 1633 (Standard Test Method for Compressive Strength of Mold Soil-Cement Cylinders), except that they were not soaked under water prior to testing. Two replicate specimens were tested at each curing time, and the maximum load sustained by each specimen was then divided by the cross-sectional area of the specimen to obtain the compressive strength.

FIGURE 3.14 Tested laboratory box specimen.

3.5 DATA ANALYSIS

Due to operator and measurement errors inherent in the testing, corrections were necessarily applied to multiple rutting records during data analysis. Recognizing that rut depth could not logically decrease with increasing numbers of wheel passes, researchers discarded individual micrometer readings that were less than previous readings. For example, if a sharp increase followed by a sharp decrease in rut depth existed with increasing numbers of wheel passes, the measurement associated with the sharp increase was considered faulty and eliminated. If one of two data entries needed to be eliminated and no engineering reason could be identified for deleting one instead of the other, the measurement that maintained the most consistent rate of increase in rut depth with increasing wheel passes was retained. Approximately 27 percent of the rutting measurements collected in each of the two HWRD data sets and 25 percent of the truck data were eliminated through this process, emphasizing the necessity of extremely meticulous data collection procedures.

Once all of the data were filtered, plots relating rut depth to CIV were created, and regression was utilized to analyze the trends and identify a threshold CIV above which the CTB should not be susceptible to unacceptable rutting. Several data transformations were considered when analyzing the data, but no significant advantages of these more complex regression models could be distinguished. Accordingly, simple linear regression was used to quantify the results of the rut testing.

3.6 SUMMARY

This research investigated the relationship between CIV and rutting susceptibility of CTB materials under early-age trafficking through both field and laboratory testing. In both cases, the testing involved forming ruts in newly constructed CTB and then measuring CIVs in the immediate vicinity of the rut locations. In the field, rut testing was performed using the HWRD, which was specially manufactured for this research, as well as a water truck and a standard pickup truck. In the laboratory, rut testing of a CTB box specimen using the HWRD was supplemented with UCS testing of CTB specimens. The collected data were analyzed using regression to identify a threshold CIV above which the CTB should not be susceptible to unacceptable rutting.

CHAPTER 4
RESULTS AND ANALYSIS

4.1 OVERVIEW

The results of field and laboratory testing are presented in the following sections. Analyses of the data follow the results. Individual rut depth and CIV measurements are included in the appendix of this report, in which hyphens indicate measurements that were necessarily eliminated during data analysis.

4.2 FIELD AND LABORATORY TESTING

Figures 4.1 and 4.2 show the results of HWRD testing in the field and in the laboratory, respectively. Figure 4.1 displays 376 data points, while Figure 4.2 displays 79 data points. As stated in Chapter 3, linear regression was utilized to quantify the relationships between rut depth and CIV in each case. Given the relative spacing of the regression lines in both Figures 4.1 and 4.2, one may conclude that successive wheel passes each cause less incremental rutting in the CTB than previous passes. This point is further illustrated in Figure 4.3, which shows rut depth versus number of wheel passes for selected field test sites representing the full range of CIVs measured in this research; the logarithmic trend lines highlight the fact that, as the number of wheel passes increases, the rate of change in rut depth decreases. The figures also show that the maximum rut depth measured in either field or laboratory rutting tests was 0.35 in.

Figure 4.4 displays the results of the laboratory UCS testing. The average UCS values computed from the replicate specimens tested at 2, 4, and 8 hours of curing were 100, 184, and 261 psi, respectively, and the corresponding average CIVs for the same time intervals were 21.1, 21.7, and 24.3. As a reference, the target 7-day UCS value currently recommended by PCA for CTB materials is 400 psi (*16, 21*).

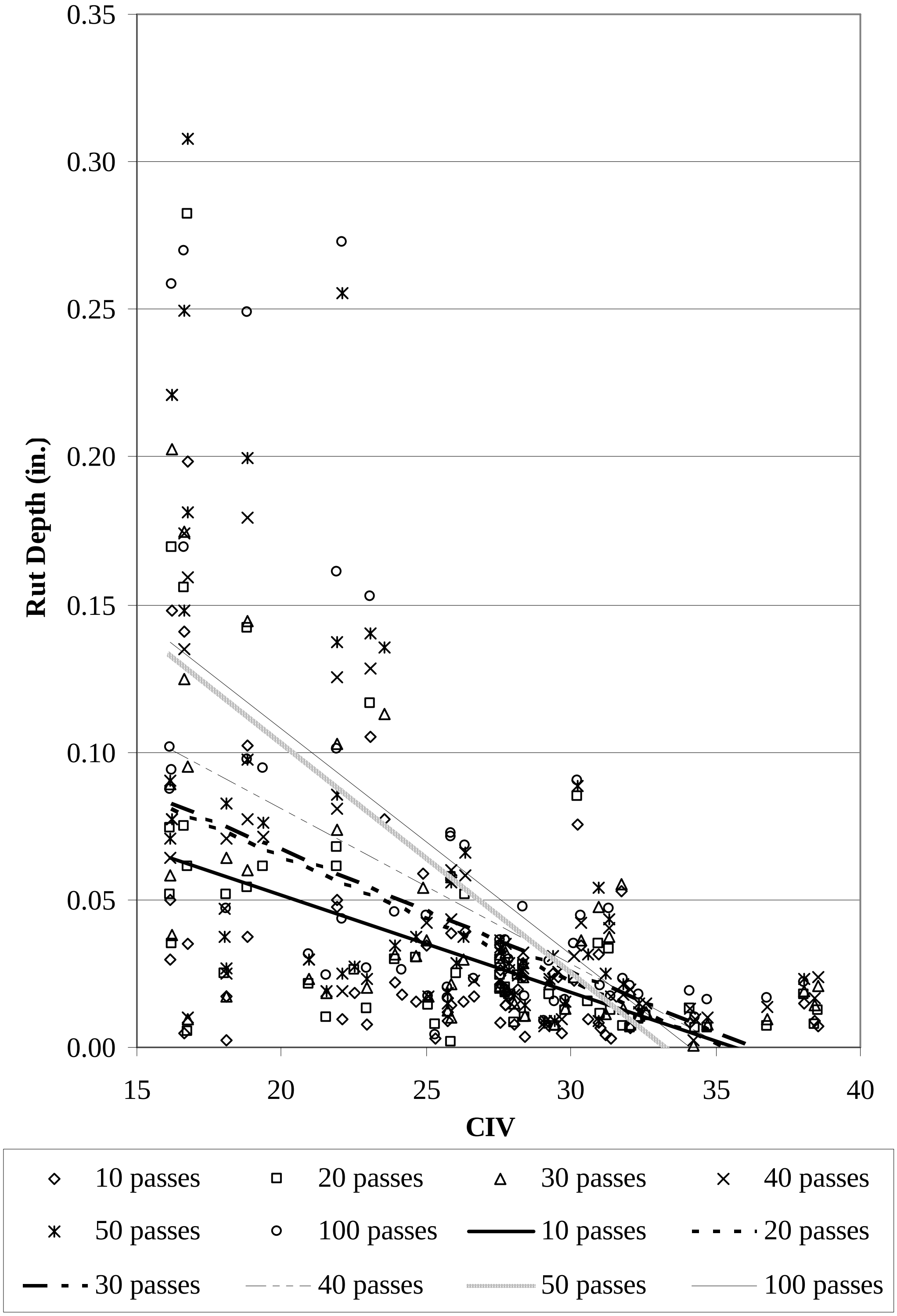

FIGURE 4.1 HWRD field data.

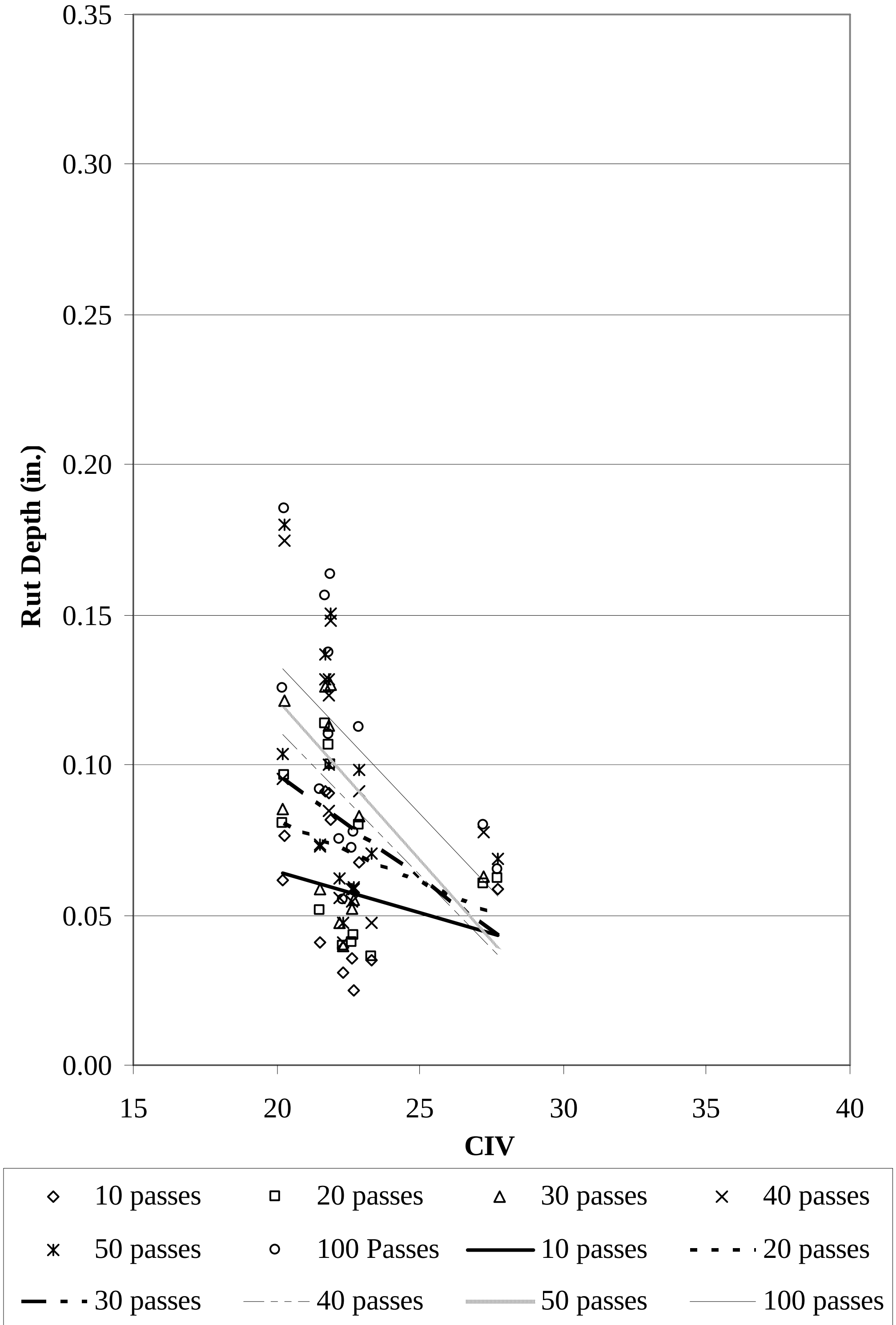

FIGURE 4.2 HWRD laboratory data.

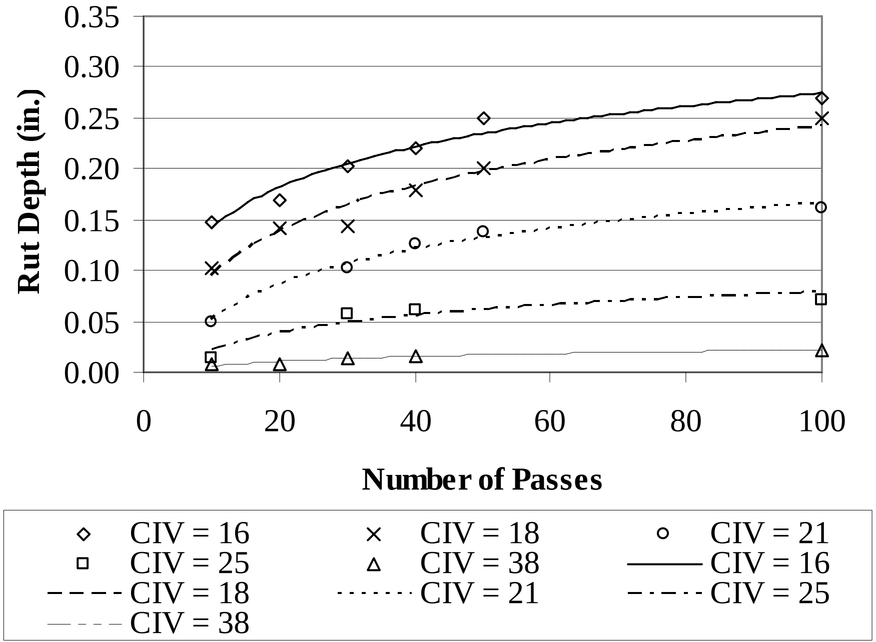

FIGURE 4.3 Rutting characteristics of selected field test sites.

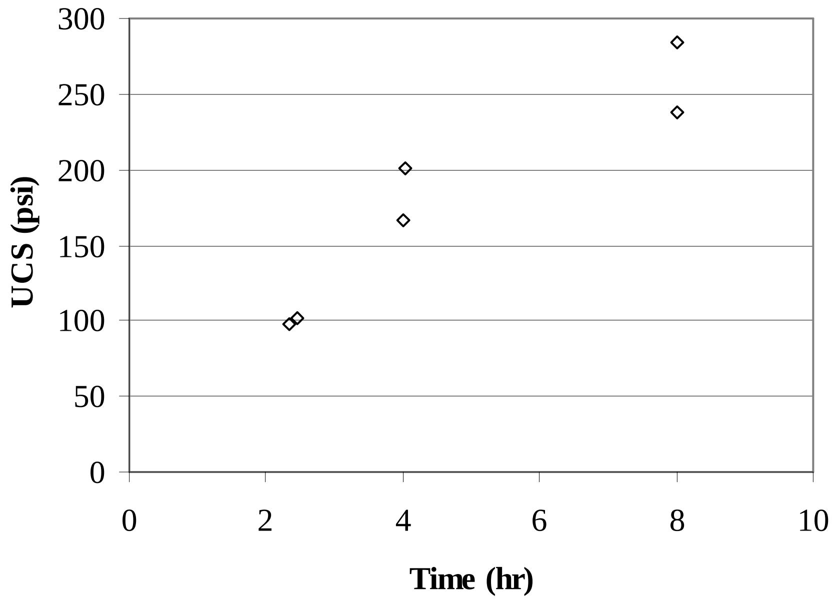

FIGURE 4.4 Compressive strengths of laboratory specimens..

Figure 4.5, which includes 10 data points, presents a summary of the data collected using a water truck and a standard pickup truck. For both truck types, rut depths were measured after 10 wheel passes in the field. Again, linear regression was utilized to define the trend in the data. Although limited in quantity, the truck data display a relationship between rut depth and CIV similar to that demonstrated in both the field and laboratory HWRD data.

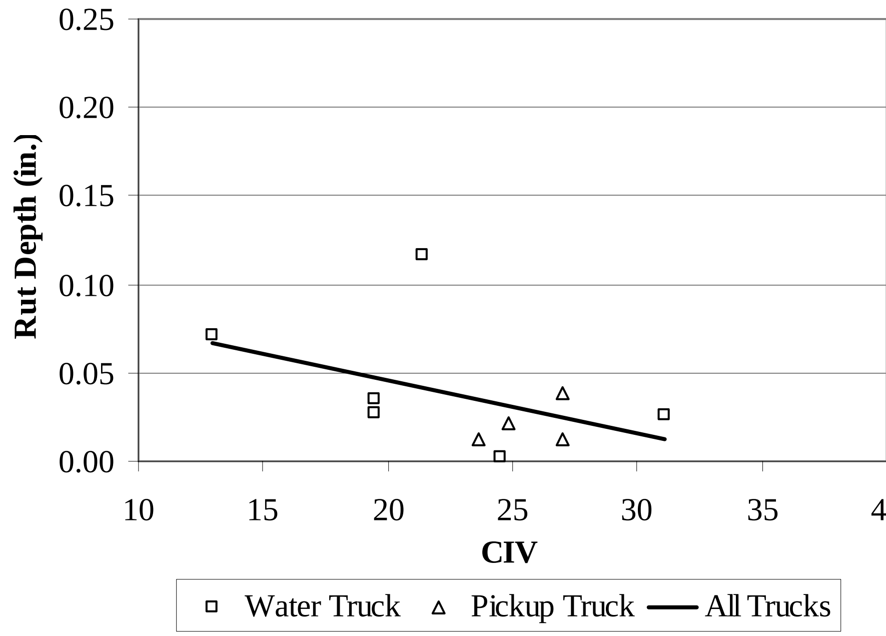

FIGURE 4.5 Truck data.

4.3 DATA ANALYSIS

In developing a recommended threshold CIV at which CTB layers may be opened to early trafficking, researchers first investigated the statistical properties of the collected data. For each data set, the equation of the regression line in the form $y = mx + b$ was determined. For each regression, the coefficient of determination (R^2) was also computed. The R^2 value describes the fraction of variation in the dependent, or response, variable that can be explained by variation in the independent variable (*32*, *33*). In addition, a *t*-test was conducted on the slope of the line in each case. The null hypothesis in the test was that the slope of the line is zero, while the alternative hypothesis was that the slope is non-zero. Table 4.1 summarizes the results of the statistical evaluations, including values of the coefficients *m* and *b*, the R^2 value, a *p*-value, and a computed CIV corresponding in each case to a rut depth of 0.0 in. When the *p*-value is less than the Type I error rate of 0.05 specified in this research as the tolerable level of error for the experimentation, the null hypothesis can be rejected, leading to acceptance of the alternative hypothesis.

The average R^2 values for the field and laboratory HWRD data are 0.3305 and 0.1608, respectively. The R^2 value associated with the truck data is 0.2061. While these comparatively low R^2 values indicate that factors beyond the aggregate stiffness measured using the CIST contribute to rut depth, the very low *p*-values associated with the field HWRD data confirm that the slopes of the regression lines are non-zero. That is, the apparent negative relationship between rut depth and CIV is of statistical significance for the field HWRD data. Although the regression lines presented in Figures 4.2 and 4.5 for the laboratory HWRD and truck data, respectively, also depict a negative relationship between rut depth and CIV, the *p*-values exceed 0.05 in all but one case, indicating that insufficient evidence exists to reject the null hypothesis that the slope of the line is zero. This result is probably attributable to the reduced number

TABLE 4.1 Statistical Results

Data Type	Wheel Passes	m	b	R^2	*p*- value	CIV at Rut Depth of 0.0 in.
Field HWRD	10	-0.0031	0.1128	0.2382	<0.0001	36.6
	20	-0.0041	0.1485	0.2835	<0.0001	36.2
	30	-0.0042	0.1524	0.3774	<0.0001	36.1
	40	-0.0053	0.1870	0.4049	<0.0001	35.3
	50	-0.0075	0.2504	0.3695	<0.0001	33.4
	100	-0.0065	0.2327	0.3093	<0.0001	35.8
Laboratory HWRD	10	-0.0027	0.1184	0.0467	0.5441	43.9
	20	-0.0041	0.1635	0.1131	0.2612	39.9
	30	-0.0069	0.2352	0.1382	0.2341	34.1
	40	-0.0098	0.3073	0.1598	0.1568	31.4
	50	-0.0104	0.3287	0.2115	0.0980	31.6
	100	-0.0101	0.3368	0.2956	0.0445	33.3
Truck	10	-0.0030	0.1065	0.2061	0.1875	35.6

of data points in those data sets and/or the small range over which the data are distributed. The average CIV corresponding to a rut depth of 0.0 in. was determined from Table 4.1 to be 35.6, suggesting that, for materials similar to the cement-treated limestone tested in this research, rutting should be negligible when the CIV exceeds about 35.

In determining a threshold CIV below which unacceptable rutting should not occur, the researchers consulted the information presented earlier in Table 2.1, examined the collected data, and considered the duration of curing that might be required in the field to achieve the threshold. A maximum rut depth of 0.1 in. was ultimately selected as a basis for analyzing the CIV data. As defined in this report, rut depths exceeding this value would therefore be considered unacceptable. Visual inspection of Figures 4.1, 4.2, and 4.5 yielded a proposed threshold CIV of 25. As noted in Chapter 2, a CIV of 25 is also within the range of CIVs typical of base layers exhibiting satisfactory long-term performance according to Clegg's research (*5*).

With respect to the amount of time that might be required for a given construction section to attain a CIV of 25 under normal curing conditions, US-91 data collected by other BYU researchers was reviewed (*2*). The CIVs of three sites, all of which were treated with 2.0 percent Portland cement and constructed using the same limestone base material utilized in this research, were monitored over time. The data, repeated in Figure 4.6 for convenience, show that an average CIV of 25 was achieved at all three sites after a curing time of between 2 and 3 days, which is 4 to 5 days shorter than the 7-day mandatory curing period specified by some agencies (*2*, *3*).

In the laboratory work conducted in this research, CIVs exceeding 25 were achieved after an 8-hour curing period. Variability in the development of strength between the CTB materials tested in the field and those tested in the laboratory is likely attributable to improved mixing quality, compaction, and curing associated with laboratory testing. As stated in Chapter 3, thorough mixing was performed in the laboratory in a portable concrete mixer, and dry densities ranging from 96 to 98 percent of MDD were achieved in compaction of the laboratory CTB box specimen; dry densities of between 85 and 88 percent of MDD were typical in the field. Furthermore, while cement hydration at the field sites may have been adversely

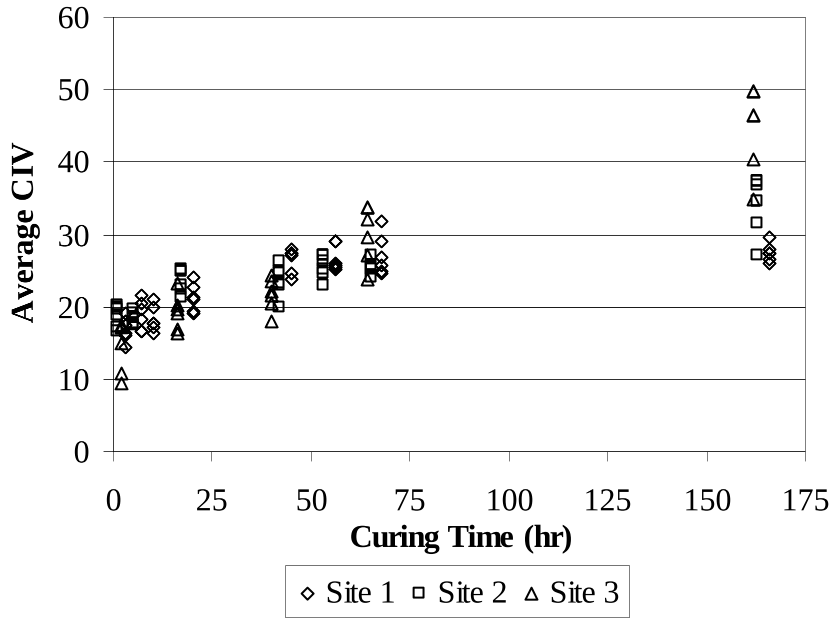

FIGURE 4.6 US-91 CIV data (*2*).

affected by the loss of mixing water due to evaporation into the air, a plastic sheet was placed over the laboratory CTB box specimen to ensure ideal curing conditions. The variability inherent in CTB construction techniques and environmental conditions emphasizes the need for a method of determining whether or not a particular CTB section can be opened to early trafficking at a particular time.

4.4 SUMMARY

From the graphs comparing rut depths and CIVs measured in both field and laboratory testing, one may conclude that successive wheel passes each cause less incremental rutting than previous passes and that CTB similar to the material tested in this research should not experience rutting at CIVs greater than about 35. The maximum rut depth measured in either field or laboratory rutting tests was just 0.35 in. in this research, probably due to the high quality limestone base material utilized to construct the CTB.

In developing a recommended threshold CIV at which CTB layers may be opened to early trafficking, researchers proposed a maximum tolerable rut depth of 0.10 in. for this project, which corresponds to a CIV of approximately 25. Because a

CIV of 25 is associated with an acceptably minimal rut depth even after 100 passes of the HWRD, is achievable within a reasonable amount of time under normal curing conditions, and is consistent with earlier research, this threshold is recommended as the minimum average value that must be attained by a given CTB construction section before it can be opened to early trafficking. Use of the proposed threshold CIV should ensure satisfactory performance of the CTB under even heavy construction traffic to the extent that the material properties do not differ greatly from those of the CTB evaluated in this research.

CHAPTER 5
CONCLUSION

5.1 SUMMARY

When available aggregate base materials exhibit inadequate strength or durability, design engineers may specify the use of cement stabilization. In order to avoid the occurrence of early-age damage, CTB materials must be allowed to cure for a period of time before the pavement can be opened to traffic. Trafficking of a cement-treated material before sufficient strength gain has occurred can lead to marring or rutting of the layer. Such damage can occur with a single pass of a heavy vehicle and only becomes more severe with repeated passes of heavy wheel loads.

To protect their investments, many agencies select curing times that overestimate the actual time needed for the CTB to gain sufficient strength that it can be opened to trafficking. This conservative approach does protect the public investment, but it also, at times, unnecessarily wastes valuable time and money on the part of the construction contractors who must wait for the specified time to expire before continuing work on the project.

As an alternative to specifying a curing time, engineers may specify field testing of CTB. Previous researchers recommended the use of the heavy CIST for assessing early-age strength gain of CTB, although no threshold CIV was developed. The specific objectives of this research were to examine the correlation between CIVs and rut depths in newly constructed CTB and subsequently establish a threshold CIV at which rutting should not occur.

The experimental work included field testing at several locations along US-91 near Smithfield, Utah, and laboratory testing at the BYU Highway Materials Laboratory. In both the field and laboratory test programs, ruts were created in CTB layers using a specially manufactured HWRD. In the field, ruts caused by repeated passes of a water truck and a standard pickup truck were also evaluated. The collected data were analyzed using regression to identify a threshold CIV above which the CTB should not be susceptible to unacceptable rutting.

5.2 FINDINGS

From the graphs comparing rut depths and CIVs measured in both field and laboratory testing, one may conclude that successive wheel passes each cause less incremental rutting than previous passes and that CTB similar to the material tested in this research should not experience rutting at CIVs greater than about 35. The maximum rut depth measured in either field or laboratory rutting tests was just 0.35 in. in this research, probably due to the high quality limestone base material utilized to construct the CTB.

5.3 RECOMMENDATIONS

In developing a recommended threshold CIV at which CTB layers may be opened to early trafficking, researchers proposed a maximum tolerable rut depth of 0.10 in. for this project, which corresponds to a CIV of approximately 25. Because a CIV of 25 is associated with an acceptably minimal rut depth even after 100 passes of the HWRD, is achievable within a reasonable amount of time under normal curing conditions, and is consistent with earlier research, this threshold is recommended as the minimum average value that must be attained by a given CTB construction section before it can be opened to early trafficking.

As described in previous research, proper sampling techniques should be followed to ensure that the CIV measurements are representative of the construction section under evaluation, and operators should be fully trained to operate the testing equipment (*2*). Use of the proposed threshold CIV should then ensure satisfactory performance of the CTB under even heavy construction traffic to the extent that the material properties do not differ greatly from those of the CTB evaluated in this research.

REFERENCES

1. Mindess, S., F. Young, and D. Darwin. *Concrete*, Second Edition. Prentice Hall, NJ, 2003.

2. Guthrie, W. S., T. B. Young, B. J. Blankenagel, and D. A. Cooley. Early-Age Strength Assessment of Cement-Treated Base Material. In *Transportation Research Record: Journal of the Transportation Research Board*, No. 1936, Transportation Research Board, National Research Council, Washington, DC, 2005, pp. 12-19.

3. Smith, B. S. *Design and Construction of Pavements in Cold Regions: State of the Practice.* M.S. thesis. Department of Civil and Environmental Engineering, Brigham Young University, Provo, UT, December 2006.

4. *Clegg Instruction Manual*. Lafayette Instrument Company, Lafayette, IN, 1996.

5. Clegg, B. Application of an Impact Test to Field Evaluation of Marginal Base Course Materials. In *Transportation Reseach Record: Journal of the Transportation Research Board*, No. 898, Transportaion Research Board, National Research Council, Washington, DC, 1985, pp. 41-48.

6. *Soil-Cement Laboratory Handbook*. Publication EB052.07S. Portland Cement Association, Skokie, IL, 1992.

7. *Guide to Full-Depth Reclamation (FDR) with Cement*. Publication EB234.01. Portland Cement Association, Skokie, IL, 2005.

8. *Soil-Cement Construction Handbook.* Publication EB003.10S. Portland Cement Association, Skokie, IL, 1995.

9. Crane, R. A., W. S. Guthrie, D. L. Eggett, and J. R. Hanson. Roughness of Flexible Pavements with Cement-Treated Base Layers. In *Transportation Research Board 85th Annual Meeting Compendium of Papers*. CD-ROM. Transportation Research Board, National Research Council, Washington, DC, January 2006.

10. Bowen, M. M., and K. Ksaibati. *Performance Evaluation of Cement-Treated Roadway Bases.* Department of Civil and Architectural Engineering, University of Wyoming, Laramie, WY, November 2000.

11. Clegg, B. An Impact Soil Test as Alternative to California Bearing Ratio. In *Proceedings of the 3rd ANZ Geomechanics Conference*, Vol. 1, Wellington, New Zealand, 1980, pp. 225-230.

12. *Clegg Impact Soil Tester Newsletter 2: Correlation with California Bearing Ratio*. Dr. Baden Clegg Pty Ltd, Western Australia, July 1986. http://www.clegg.com.au/information_list12.asp. Accessed April 5, 2007.

13. *Clegg Impact Soil Tester Newsletter 18: Testing of Flexible Road Pavements with the 20 kg Clegg Imact Soil Tester*. Dr. Baden Clegg Pty Ltd, Western Australia, August 1997. http://www.clegg.com.au/newslett2.asp. Accessed April 5, 2007.

14. *Clegg Impact Soil Tester Newsletter 15: Testing of Gravel and Crushed Rock Roads with the 20 kg Clegg Hammer.* Dr. Baden Clegg Pty Ltd, Western Australia, February 1995. http://www.clegg.com.au/20kginfo.asp. Accessed April 5, 2007.

15. *Clegg Impact Soil Tester Newsletter 14: Clegg Hammer Modulus (CHM).* Dr. Baden Clegg Pty Ltd, Western Australia, August 1999. http://www.clegg.com.au/information_list3.asp. Accessed April 5, 2007.

16. Brown, A. V. *Cement Stabilization of Aggregate Base Material Blended with Reclaimed Asphalt Pavement*. M.S. thesis. Department of Civil and Environmental Engineering, Brigham Young University, Provo, UT, August 2006.

17. Cooley, D. A. *Effects of Reclaimed Asphalt Pavement on Mechanical Properties of Base Materials*. M.S. thesis. Department of Civil and Environmental Engineering, Brigham Young University, Provo, UT, December 2005.

18. Lotfi, H., and M. W. Witczak. Dynamic Charaterization of Cement-Treated Base and Subbase Materials. In *Transportation Reseach Record: Journal of the Transportation Research Board*, No. 1031, Transportation Research Board, Washington, DC, 1983, pp. 174-181.

19. Akili, W., and C. L. Monismith. Permanent Deformation Characteristics of Cement-Emulsion Stablized Sand. In *Asphalt Paving Technology*, Vol 47, 1978, pp. 281-301.

20. Guthrie, W. S., R. D. Lay, and A. J. Birdsall. Effect of Reduced Cement Contents on Frost Heave of Silty Soil: Laboratory Testing and Numerical Modeling. In *Transportation Research Board 86th Annual Meeting Compendium of Papers*. CD-ROM. Transportation Research Board, National Research Council, Washington, DC, January 2007.

21. Guthrie, W. S., A. V. Brown, and D. L. Eggett. Cement Stabilization of Aggregate Base Material Blended with Reclaimed Asphalt Pavement. In *Transportation*

Research Board 86th Annual Meeting Compendium of Papers. CD-ROM. Transportation Research Board, National Research Council, Washington, DC, January 2007.

22. Guthrie, W. S., and T. B. Young. Evaluation of Transition Cement for Stabilization of Frost-Susceptible Base Material in Conjunction with Full-Depth Recycling in Weber Canyon, Utah. In *Proceedings of the American Society of Civil Engineers 13th International Conference on Cold Regions Engineering*. CD-ROM. Orono, ME, July 2006.

23. Miller, H., W. S. Guthrie, M. Kestler, and C. Carbo. Cement Treatment of Frost-Susceptible New England Base Materials Blended with Reclaimed Asphalt Pavement. In *Proceedings of the American Society of Civil Engineers 13th International Conference on Cold Regions Engineering*. CD-ROM. Orono, ME, July 2006.

24. Guthrie, W. S., S. D, Sebesta, and T. Scullion. *Selecting Optimum Cement Contents for Stabilizing Aggregate Base Materials.* Report 7-4920-2. Texas Transportation Institute, Texas A&M University System, College Station, TX, February 2002.

25. Gaspard, K. J. Evaluation of Cement Treated Base Courses. Publication 00-1TA. Louisiana Transportation Research Center, Louisiana Department of Transportation and Development, Baton Rouge, LA, December 2000.

26. Mahasantipiya, S. Performance Analysis of Bases for Flexible Pavement. *Dissertation Abstracts International,* Vol. 61/07-B, 2000, pp. 3736.

27. Benkelman, A. C., R. I, Kingman, and H. M. Schmitt. Performance of Treated and Untreated Bases. *Highway Research Board Special Reports*, No. 73, 1962, pp. 242-255.

28. Asphalt Pavement Technology, Bituminous Mixtures Laboratory Equipment, Hamburg Wheel Tracking Device. Federal Highway Administration, U.S. Department of Transportation, Washington, DC. http://www.fhwa.dot.gov/pavement/asphalt/labs/mixtures/hamburg.cfm. Accessed April 9, 2007.

29. Huang, Y. H. *Pavement Analysis and Design*, Second Edition. Prentice Hall, Upper Saddle River, NJ, 2004.

30. Collins, R., D. Watson, B. Campbell. How Georgia Predicts Asphalt Rutting. *Better Roads*, Vol. 65, No. 8, 1995, pp. 27-28.

31. Google Maps Homepage. http://maps.google.com/maps?ie=UTF-8&oe=UTF-8&hl=en&tab=wl&q=. Accessed April 19, 2007.

32. Ramsey, F. L., and D. W. Schafer. *The Statistical Sleuth: A Course in Methods of Data Analysis*, Second Edition. Duxbury, Pacific Grove, CA, 2002.

33. Ott, R. L., and M. Longnecker. *An Introduction to Statistical Methods and Data Analysis*, Fifth Edition. Duxbury, Pacific Grove, CA, 2001.

APPENDIX

TABLE A.1 HWRD Field Data

Site	Wheel Path	Rut Depth (in.)						Average CIV
		Wheel Passes						
		10	20	30	40	50	100	
1	Left	0.002	-	0.170	0.025	0.027	0.047	18.1
	Right	0.017	0.052	0.064	0.071	0.082	-	18.1
2	Left	0.102	0.142	0.144	0.180	0.200	0.249	18.8
	Right	0.038	0.054	0.600	0.077	0.097	0.097	18.8
3	Left	0.030	0.052	0.580	0.064	0.070	0.087	16.2
	Right	0.050	0.074	0.089	-	0.090	0.102	16.2
4	Left	-	-	-	-	0.256	0.273	22.1
	Right	0.010	-	-	0.019	0.025	0.043	22.1
5	Left	0.050	0.062	0.073	0.081	0.086	0.101	21.9
	Right	0.047	0.068	0.103	0.125	0.137	0.161	21.9
6	Left	0.035	0.610	0.095	0.160	0.182	-	16.8
	Right	0.198	0.282	-	-	0.308	-	19.8
7	Left	0.015	-	0.021	0.043	0.056	0.071	25.8
	Right	0.039	0.058	0.058	0.060	-	0.072	25.8
8	Left	0.141	0.156	0.175	0.174	0.249	0.270	16.6
	Right	0.005	0.075	0.125	0.135	0.148	0.169	16.6
9	Left	-	0.035	0.038	0.077	0.077	0.094	16.2
	Right	0.148	0.170	0.203	0.221	0.221	0.259	16.2
10	Left	0.023	0.023	-	0.031	-	0.035	30.1
	Right	0.004	-	0.011	0.025	-	0.030	31.2
11	Left	-	0.010	0.019	-	0.019	0.024	21.6
	Right	0.014	0.019	0.019	-	0.020	0.023	27.8
12	Left	0.008	0.013	-	0.013	-	0.019	34.1
	Right	-	0.008	-	-	-	-	32.5
13	Left	0.003	-	-	-	-	0.004	25.3
	Right	0.012	0.018	0.013	0.015	0.017	0.019	25.8
14	Left	0.015	0.015	0.019	-	0.023	0.022	38.1
	Right	0.009	0.300	-	0.031	-	0.047	30.6
15	Left	0.022	0.013	0.032	-	0.034	0.046	23.9
	Right	0.008	0.006	0.020	0.023	0.270	-	22.9
16	Left	-	-	0.008	0.010	-	0.016	34.7
	Right	0.018	-	-	-	0.260	0.029	24.1
17	Left	0.059	-	0.054	-	-	-	24.9
	Right	0.028	0.007	-	0.036	0.036	-	27.5
18	Left	-	0.011	0.008	0.009	0.009	0.015	29.5
	Right	0.006	0.008	-	-	0.021	-	31.0
19	Left	0.008	-	0.015	0.014	0.018	-	28.0
	Right	0.025	0.085	-	0.031	-	0.039	29.4
20	Left	0.075	0.018	-	-	0.089	0.090	30.2
	Right	0.017	0.061	0.026	0.028	0.030	0.036	27.9

TABLE A.1 (Continued)

Site	Wheel Path	Rut Depth (in.)						Average CIV
		Wheel Passes						
		10	20	30	40	50	100	
21	Left	-	0.026	-	0.071	0.076	0.094	19.4
	Right	0.019	0.013	-	0.028	-	0.038	22.5
22	Left	0.007	0.030	0.021	0.024	-	-	38.6
	Right	0.026	-	0.032	-	-	0.032	27.6
23	Left	-	0.051	-	-	-	-	25.0
	Right	0.039	0.025	0.058	0.066	0.068	0.082	26.3
24	Left	-	0.117	-	0.047	0.037	0.052	18.0
	Right	0.105	0.024	0.129	0.141	0.153	0.189	23.1
25	Left	0.020	0.014	-	-	0.024	0.025	28.2
	Right	0.009	0.005	-	0.019	0.020	0.031	25.7
26	Left	-	0.113	0.010	0.010	-	0.015	16.8
	Right	0.077	-	-	0.136	-	0.146	23.5
27	Left	0.015	0.036	0.030	-	0.037	0.063	26.3
	Right	0.035	0.025	0.042	-	0.044	0.075	25.0
28	Left	-	0.036	-	-	0.029	0.029	26.1
	Right	0.035	0.011	0.042	-	0.044	0.075	30.4
29	Left	-	-	0.012	0.015	-	-	32.6
	Right	0.008	-	0.009	-	-	-	29.1
30	Left	0.005	-	-	0.010	-	0.013	29.7
	Right	0.024	0.002	0.026	-	-	0.028	29.5
31	Left	-	0.055	0.010	-	-	-	25.9
	Right	0.053	0.031	-	-	-	0.064	31.8
32	Left	0.016	0.024	0.031	-	0.038	-	24.6
	Right	-	-	0.029	0.027	0.047	-	28.4
33	Left	0.017	-	-	0.023	0.023	0.050	26.6
	Right	0.008	0.008	-	0.009	-	-	31.0
34	Left	0.009	-	0.014	0.017	-	0.022	38.4
	Right	-	-	0.007	0.008	0.009	0.011	29.1
35	Left	-	0.009	0.000	0.002	-	-	34.2
	Right	0.007	-	0.014	-	0.017	-	36.8
36	Left	0.021	0.024	0.032	0.034	-	-	27.5
	Right	0.007	0.013	0.018	0.021	0.023	0.024	31.8
37	Left	0.003	0.013		0.017	0.017	0.018	31.4
	Right	0.018	0.021	0.022	0.023	0.029	0.030	29.3
38	Left	0.015	0.020	0.032	0.035	0.036	0.040	27.7
	Right	0.010	0.011	0.012	0.015	0.018	0.023	32.3
39	Left	0.024	0.028	0.028	0.032	-	0.041	28.4
	Right	0.033	0.037	0.041	0.043	0.047	0.050	31.3
40	Left	0.006	0.006	0.008	0.019	0.021	0.026	32.1
	Right	0.013	0.013	-	0.015	0.016	0.017	29.8

TABLE A.1 (Continued)

Site	Wheel Path	Rut Depth (in.)						Average CIV
		Wheel Passes						
		10	20	30	40	50	100	
41	Left	0.008	0.019	0.021	0.023	0.035	0.036	27.5
	Right	0.021	0.023	0.029	0.030	0.032	0.037	21.0
42	Left	0.004	0.010	0.011	0.014	0.017	0.019	28.4
	Right	0.014	0.017	0.017	-	0.018	0.030	25.1
43	Left	0.032	0.035	0.047	0.054	-	0.057	30.9
	Right	0.006	-	0.009	-	0.010	-	34.3

TABLE A.2 HWRD Laboratory Data

Site	Wheel Path	Rut Depth (in.)						Average CIV
		Wheel Passes						
		10	20	30	40	50	100	
1	Left	-	-	-	0.085	0.100	0.110	21.8
	Right	-	-	-	-	-	-	20.8
2	Left	0.041	0.052	0.059	0.073	0.074	0.092	21.5
	Right	0.061	0.081	0.085	0.095	0.104	0.126	20.2
3	Left	0.031	0.040	0.040	0.041	0.048	0.055	22.3
	Right	-	0.061	0.063	0.078	-	0.080	27.2
4	Left	0.077	0.096	0.122	0.175	0.180	0.185	20.3
	Right	0.082	0.100	0.127	0.148	0.151	0.163	21.9
5	Left	-	-	0.047	0.056	0.062	0.075	22.2
	Right	0.067	0.080	0.083	0.091	0.098	0.113	22.9
6	Left	0.035	0.041	0.052	0.055	0.058	0.072	22.6
	Right	0.059	0.062	-	-	0.069	0.065	27.7
7	Left	-	-	-	-	-	-	20.5
	Right	-	-	-	-	-	-	21.4
8	Left	0.090	0.107	0.113	0.123	0.129	0.138	21.8
	Right	0.091	0.114	0.126	0.128	0.137	0.157	21.7
9	Left	0.025	0.043	0.055	0.059	0.059	0.077	22.7
	Right	0.035	0.036	-	0.047	0.071	-	23.3

TABLE A.3 Truck Data

Truck Type	Wheel Path	Rut Depth (in.)	Average CIV
Water Truck	1	0.027	19.5
	2	0.035	19.5
	3	0.071	13.0
	4	0.117	21.4
	5	0.003	24.5
	6	0.026	31.1
Pickup Truck	1	0.013	23.7
	2	0.021	24.8
	3	0.013	27.0
	4	0.038	27.0